Magnetic Raman scattering of insulating cuprates

J. Eroles, C. D. Batista, S. B. Bacci, and E. R. Gagliano
Comisión Nacional de Energía Atómica, Centro Atómico Bariloche e Instituto Balseiro, 8400 S.C. de Bariloche (RN), Argentina
(Received 5 November 1997)

We study the B_{1g} and A_{1g} Raman profiles of M_2CuO_4 (with $M=$La, Pr, Nd, Sm, Gd), $Bi_2Sr_2Ca_{0.5}Y_{0.5}Cu_2O_{8+y}$, $YBa_2Cu_3O_{6.2}$, and $PrBa_2Cu_{2.7}Al_{0.3}O_7$ insulating cuprates within the Loudon-Fleury theory, in the framework of an extended Hubbard model for moderate on-site Coulomb interaction U. We calculate the nonresonant contribution to these Raman profiles by using exact diagonalization techniques and analyze two types of contributing mechanisms to the line shapes: four-spin cyclic exchange and spin-phonon interactions. Although these interactions contribute to different parts of the spectra, together, they account for the enhanced linewidth and asymmetry of the B_{1g} mode, as well as the non-negligible intensity of the A_{1g} Raman line observed in these materials. [S0163-1829(99)00901-7]

I. INTRODUCTION

Inelastic Raman and neutron-scattering experiments on insulating cuprates provide information about the spin dynamic of the CuO_2 planes of high-T_c precursors.[1] The observed short- and long-wavelength low-energy excitations have been described using the two-dimensional spin-$\frac{1}{2}$ antiferromagnetic Heisenberg model (AFH), and the standard theory of Raman scattering based on the Loudon-Fleury[2] (LF) coupling between the light and the spin system. Within this theoretical scheme, the value of the Cu-Cu exchange constant J has been estimated from the first moment M_1 of the B_{1g} Raman line and, in virtual agreement, from neutron-scattering measurements of the spin velocity. For insulating materials having the Cu atom on different chemical environments, the estimated value of J results in the range $\sim(0.10-0.14)$ eV.

Within the AFH framework, numerical and analytical calculations have been able to describe the temperature dependence of the spin-spin correlation length obtained from neutron-scattering data,[3,4] the temperature dependence of the spin-lattice-relaxation rate $1/T_1$ measured by nuclear magnetic resonance,[5,6] and a prominent structure, ascribed to two-magnon scattering, of the B_{1g} Raman line.[7–11] Although all these theoretical results suggest the AFH on the square lattice as a *very good starting point* for describing the spin dynamic of the insulating cuprates, some features of the Raman lines remain to be explained within the LF theory. In particular, the AFH-LF failure to describe the B_{1g} spectral shape and its enhanced width is not yet understood, and of course, the AFH-LF cannot reproduce a nonvanishing A_{1g} response.

The shape of the B_{1g} line presents some characteristic features common to several insulating cuprates. In fact, at room temperature, a *very similar* line shape has been observed for all members of the M_2CuO_4 series ($M=$La, Pr, Nd, Sm, Gd), $Bi_2Sr_2Ca_{0.5}Y_{0.5}Cu_2O_{8+y}$ (BSCYCO), $YBa_2Cu_3O_{6.2}$, and $PrBa_2Cu_{2.7}Al_{0.3}O_7$ (PRBACUALO).[12–16] In all cases, the line extends up to $\sim 8J$, which in the Ising limit, can be ascribed to multimagnon excitations involving 16 spins. Unfortunately, calculations on the AFH show a negligible contribution of multimagnon processes not only for the Raman line but also for the spin structure factor at the antiferromagnetic wave vector. Another feature is a very intensive peak located at $\omega\sim 3J$, identified as two-magnon scattering.[7–10] Now, it is believed that the asymmetry of the line originates on a second hidden peak on the high-energy side of the spectrum at $\omega\sim 4J$ whose intensity is $\sim 25\%$ smaller than the intensity of the two-magnon peak.[14] In the Ising limit, the energy of these magnetic excitations corresponds to four-magnon scattering. For the AFH model, they give a very small contribution to the intensity of the spectrum. On other geometries interesting features also appear. The A_{1g} line has a maximum at a slightly high frequency with respect to the two-magnon peak,[17] while for the A_{2g} and B_{2g} symmetries the center of the spectrum is located at $\omega\sim 5J$ and $\omega\sim 4J$, respectively.[18] Finally, a slight temperature dependence of the scattering intensities of the B_{1g} line in the insulating cuprates has been found. In fact, the rise in temperature from 30 to 273 K causes the two-magnon peak intensity to decrease by only $\sim 10\%$, in contrast to $\sim 50\%$ for the $S=1$ system La_2NiO_4.[12] Consistently, previous calculations show a weak temperature dependence of the B_{1g} spectrum for $T<J$ (Ref. 19) for the spin-$\frac{1}{2}$ AFH model, which in turn suggests the importance of short-range spin-spin correlations.

In the Fleury-Loudon theory, the state emerging from the application of the current operator on the ground state is considered as an eigenstate. In this intermediate eigenstate, the electron and the hole, produced by the photon scattering, are very close in real space, creating a charge-transfer exiton, and the individual propagation of each particle is neglected. This approximation could be appropriated for the case of the cuprates due to the presence of an electron-electron interaction (U_{pd}) between nearest-neighbor sites (oxygen and copper sites). This interaction, not included in the Hubbard Hamiltonian, is important to describe the charge excitations of the cuprates and induces an attractive interaction between the hole and the electron.[20] Due to this interaction, the hole and the electron are close in space and there is not free individual propagation of them.[21] Furthermore, the disorder present in the cuprates[22] tends to localize the electron-hole pairs. Chubukov and Frenkel tried to include the resonant effects in the frame of the one-band Hubbard model.[23]

 ©1999 The American Physical Society

Schönfeld *et al.*[24] calculated the resonant contributions but they could not properly describe the B_{1g} profile, and the observed A_{1g} line remains to be explained. In both cases, they did not include the effect of the U_{pd} interaction to describe the charge excitations and considered that the electron and the hole propagate individually. For the reasons given above, we think that the Fleury-Loudon theory is an appropriated framework to describe the Raman spectra of the cuprates.

Even when the resonant effects may be needed to explain the dependence of the Raman spectra on the incoming laser frequency, the main features of the line studied in our work persist over the wide range of frequencies used in the experiments[12,13,16,17,25,26] and are essentially the same as that out of resonance. This point is shown in, e.g., the recent work in $PrBa_2Cu_{2.7}Al_{0.3}$,[16] where the Raman spectra out of resonance was measured and the main features of the B_{1g} line shape remain unaltered. Besides, the LF theory has been the standard framework to describe the Raman spectra of other antiferromagnetic $S=1/2$ compounds.[27,28] So, it is an interesting issue whether the persistent aspects of the Raman line can be well described within the LF theory with an appropriate model.

Previous theoretical work using LF theory tackled the problem of the line's shape by using series expansions, variational Monte Carlo, interacting spin waves, and exact diagonalization techniques on small clusters.[7–11]

Different theoretical scenarios have been proposed for describing the anomalously enhanced width of the B_{1g} line, and although at a first sight, quantum fluctuations could be the main contribution to the width of the B_{1g} line, this last hypothesis has been rejected after measurements on the $S=1$ system $NiPS_3$ for which a relative width comparable to the insulating cuprates has been observed.[29] A different proposal has been motivated by the temperature dependence of the two-magnon peak, namely, an increase of the Raman linewidth with increasing temperatures.[30] This has been considered as a strong indication of a phonon mechanism for the line's broadening and its effect has been analyzed through a non-uniform renormalization of the exchange constant J.[31] Another argument which supports the phonon mechanism is that although the second cumulant M_2 of the B_{1g} Raman spectrum is almost J independent for the materials mentioned above, its exchange constant changes by $\sim 20\%$. This indicates a linewidth dominated by nonmagnetic contributions such as intrinsic disorder of the spin lattice, defects or phonons. Of course, this does not rule out other magnetic mechanism providing scattering at frequencies higher than the two-magnon peak.

So far, the phonon mechanism alone is insufficient to describe the line asymmetry due to important contributions of four-magnon scattering.[30] This requires us to go beyond the minimal AFH model. An effective description of the insulating cuprates based on the single-band Hubbard model[32] recently appeared, giving a theoretical framework with which to go beyond the AFH model and provides additional multispin interactions which finally could contribute not only to the Raman spectra but also to the midinfrared phonon-assisted optical conductivity.[33] In this work, we extend previous calculations of the B_{1g} and A_{1g} lines based on the minimal AFH model by including multispin and spin-phonon interactions. We calculate the Raman spectra on finite-size systems using the now standard Lanczos method[34] for the series of materials mentioned above. Since inelastic light-scattering measurements probe short-wavelength spin fluctuations, we expect finite-size effects to be small.[35] We find that two mechanisms, multispin and spin-phonon interactions, contribute to the width and shape of the B_{1g} Raman line, and at the same time, allow an otherwise forbidden A_{1g} response.

II. RAMAN SPECTRA AND EFFECTIVE SPIN MODEL

The scattering of light from insulating antiferromagnets at energies smaller than the charge-transfer gap $\sim(1.5-2)$ eV can be described phenomenologically, by introducing a Raman operator, based on the symmetries of the magnetic problem. For the one-dimensional irreducible representations of the square, these operators are given by

$$O_{B_{1g}}=\sum_{\mathbf{i}} \vec{S}_{\mathbf{i}}\cdot(\vec{S}_{\mathbf{i}+\mathbf{e_x}}-\vec{S}_{\mathbf{i}+\mathbf{e_y}}),$$

$$O_{A_{1g}}=\sum_{\mathbf{i}} \vec{S}_{\mathbf{i}}\cdot(\vec{S}_{\mathbf{i}+\mathbf{e_x}}+\vec{S}_{\mathbf{i}+\mathbf{e_y}}),$$

$$O_{B_{2g}}=\sum_{\mathbf{i}} (\vec{S}_{\mathbf{i}}\cdot\vec{S}_{\mathbf{i}+\mathbf{e_x}+e_y}-\vec{S}_{\mathbf{i}+e_x}\cdot\vec{S}_{\mathbf{i}+\mathbf{e_y}}),$$

$$O_{A_{2g}}=\sum_{\mathbf{i}} \epsilon_{\mu\nu}\vec{S}_{\mathbf{i}}\cdot(\vec{S}_{\mathbf{i}+\mathbf{e}_\mu}\times\vec{S}_{\mathbf{i}+\mathbf{e}_\nu}).$$

where $\mu=\pm x,\pm y$, and $\epsilon_{\mu\nu}=-\epsilon_{\nu\mu}=-\epsilon_{-\mu\nu}$. Here $\mathbf{e_x}$ and $\mathbf{e_y}$ denote unit vectors in x,y directions of a square lattice. The Raman Hamiltonian is proportional to one of these operators, being the prefactor matrix elements of the dipolar moment, and therefore, depends on microscopic details of the system. Here, we will assume them all equal to one and therefore we will be unable to compare the relative intensities of spectra of different symmetries. Microscopically, these Raman operators can be derived from the theory of Raman scattering in Mott-Hubbard systems.[36] In the strong-coupling limit of the Hubbard model, they appear quite naturally as the leading-order contributions in an expansion in $\Delta=t/(U-\omega)$. Of course, for the two-dimensional (2D) AFH model, the $O_{A_{1g}}$ operator commutes with the Hamiltonian, so the A_{1g} response vanishes at the lowest order and terms of order Δ^3 are required to have a small but finite response.

The Raman spectrum $R_\Gamma(\omega)$ at $T=0$, is given by

$$R_\Gamma(\omega)=\sum_n |\langle\phi_0|O_\Gamma|\phi_n\rangle|^2\delta(\omega-E_n+E_0),$$

where Γ is A_{1g}, B_{1g}, A_{2g} or B_{2g}, $|\phi_0\rangle$ is the ground state, E_0 is the ground-state energy, and $|\phi_n\rangle$ is an excited state of the system with energy E_n. The spectrum $R_\Gamma(\omega)$ can be obtained from a continued fraction expansion of the diagonal matrix element of the resolvent operator $1/(\omega+E_0+i\delta-H)$ between the state $O_\Gamma|\phi_0\rangle$. Here δ is a small imaginary part added to move the poles away from the real axis.[34]

TABLE I. Values of the single-band parameters for the different insulators.

	$YBa_2Cu_3O_{6.2}$	Pr_2CuO_4	Nd_2CuO_4	Sm_2CuO_4	La_2CuO_4	Gd_2CuO_4	BSCYCO	PRBACALO
U/t	9.5	9.5	9.5	9.5	10.5	9.5	10.5	9.5
t'/t	0.28	0.30	0.28	0.30	0.30	0.30	0.30	0.30
t (eV)	0.40	0.42	0.42	0.435	0.475	0.435	0.45	0.37
J (eV)	0.138	0.145	0.145	0.150	0.154	0.150	0.146	0.140

Let us describe first the B_{1g} Raman spectrum of the 2D antiferromagnetic Heisenberg model. It has mainly two contributions: (a) a very strong *two-magnon* structure located at $\omega\sim 3J$ and (b) a weaker *four-magnon* processes at higher energies.

In a recent work, Sandvik *et al.*[11] calculated numerically the Heisenberg B_{1g} spectrum for lattices up to 6×6 sites. They found a change in the strong structure at $\omega\sim 3J$ in the exact spectrum going from 4×4, with a single two-magnon dominant peak, to 6×6, where two equal-sized peaks appear. Unfortunately this is the bigger system available nowadays and it is not clear if these two peaks are not a spurious characteristic of this cluster since this kind of structure is not observed in bigger systems calculated with Monte Carlo max entropy.[11] They concluded that the Heisenberg model cannot describe the broad B_{1g} spectrum and, of course, it gives a zero A_{1g} profile even for that size of clusters. The four-spin excitations are generated by flipping two pairs of spins of the Néel background in a plaquete or in a column with an energy cost of $4J$ and $5J$, respectively. The intensity of these high-frequency processes is *very small* $<10\%$,[8,35] and cannot account for the asymmetry observed for this mode[37] on the high-frequency side of the spectrum. Since a distinct shoulder appears at $\omega\sim 4J$, it has been proposed that the four-magnon channel is enhanced by four-spin cyclic exchange interactions.[12] In fact, finite cluster calculations[38,39] for the undoped compound have shown that although within the CuO_2 planes the leading term in the effective spin Hamiltonian is the antiferromagnetic Heisenberg exchange interaction, other terms are required to describe the low-energy spin excitations. These higher-order terms appear naturally by performing a canonical transformation up to fourth order on the Hubbard model.[40] A single-band Hubbard model can simultaneously describe the low-energy charge and spin responses of insulating $Sr_2CuO_2Cl_2$.[32] Hence, our starting model to describe the spin dynamic of all the compounds mentioned before, is an extended Hubbard Hamiltonian, including next-nearest-neighbor (NNN) hopping t'. By means of a canonical transformation to fourth order in t and second order in t', the effective spin Hamiltonian is written as follows:

$$H_{\rm eff}=J\sum_{i,\delta}\left(\mathbf{S}_i\mathbf{S}_{i+\delta}-\frac{1}{4}\right)+J'\sum_{i,\delta'}\left(\mathbf{S}_i\mathbf{S}_{i+\delta'}-\frac{1}{4}\right)$$
$$+K\sum_{\langle i,j,k,l\rangle}(\mathbf{S}_i\mathbf{S}_j)(\mathbf{S}_k\mathbf{S}_l)+(\mathbf{S}_i\mathbf{S}_l)(\mathbf{S}_j\mathbf{S}_k)-(\mathbf{S}_i\mathbf{S}_k)(\mathbf{S}_j\mathbf{S}_l)$$

with $J=4t^2/U-64t^4/U^3$, $J'=4t'^2/U+4t^4/U^3$, and $K=80t^4/U^3$. $\delta(\delta')$ runs over NN (NNN) and $\langle i,j,k,l\rangle$ means the sum over groups of four spins in a unit square. The effect of the cyclic exchange interaction on the antiferromagnetic ground state of the 2D Heisenberg model has been studied showing that for small values of K/J, the antiferromagnetic phase is stable.[41] The staggered magnetization increases as K/J is increased, has a maximum at ~ 0.75, and then decreases showing a transition to a spin-canted region. In particular, for the value of K estimated for the cuprates, the system is still in the antiferromagnetic phase and its staggered magnetization is $m_{\rm st}\sim 0.58$. The reduction of the three-band model onto the single-band Hubbard model for realistic values of the multiband parameters, indicates that the effective hopping t is bounded between 0.3 and 0.5 eV, while $U/t\sim 7-10$.[42] Furthermore, the derivation of the one-band Hubbard Hamiltonian given by Simón and Aligia (see Ref. 42) for the parameters obtained from local-density approximation calculations for La_2CuO_4, gives $t\sim 0.45$ eV, $U/t\sim 7.6$, $t'/t\sim 0.15$. Deviations from these values are expected for different materials, in particular, for the values of the long-range hoppings. In Table I, we show the values of the parameters for the eight systems studied in this work.

III. RESULTS

Let us examine first the role of multispin interactions on the spectra. Figure 1 shows the calculated Raman spectrum at different symmetries for $U=9.5t$ and $t'=0.28t$. The B_{1g} line shows the same features as for the Heisenberg model, being the main difference the gain of spectral weight at high frequencies, Fig. 1(a). The four-magnon processes are now enhanced having a relative intensity to the two-magnon peak of $\sim 20\%$. This is in agreement with Ref. 14, where it has been found that the deviation from the symmetric part of the B_{1g} mode is mainly due to a peak located at $\omega\sim 4J$ whose intensity is about 20% of the two-magnon peak. For the A_{2g} and B_{2g} modes, Fig. 1(c), the center of gravity of the spectra agree rather well with the experimental data.[18]

However, calculations for the A_{1g} line, Fig. 1(b), shows that the maximum is shifted by $\sim J$ respect to the two magnon peak, in disagreement with the experimental shift. Although the four-spin cyclic exchange interaction provides a mechanism for some features of the B_{1g} mode and yields responses in the correct frequency range for the A_{2g} and B_{2g} lines, it does not give correctly the frequency range for the A_{1g} spectrum neither the full linewidth of the B_{1g} line. As was mentioned before, this can be due to sample inhomogeneities, additional strong interactions with the spin excitations and/or disorder. Among all of them, the spin-phonon interaction seem to be the best candidate.

The occurrence of a strong Peierls-type Fermi-surface instability involving breathing-type displacements of the oxygen atoms of the CuO_2 planes suggests that spin-phonon interactions could contribute to the damping of the spin excitations of the insulating compounds. The in-plane phonon modes have small energy compared to the exchange

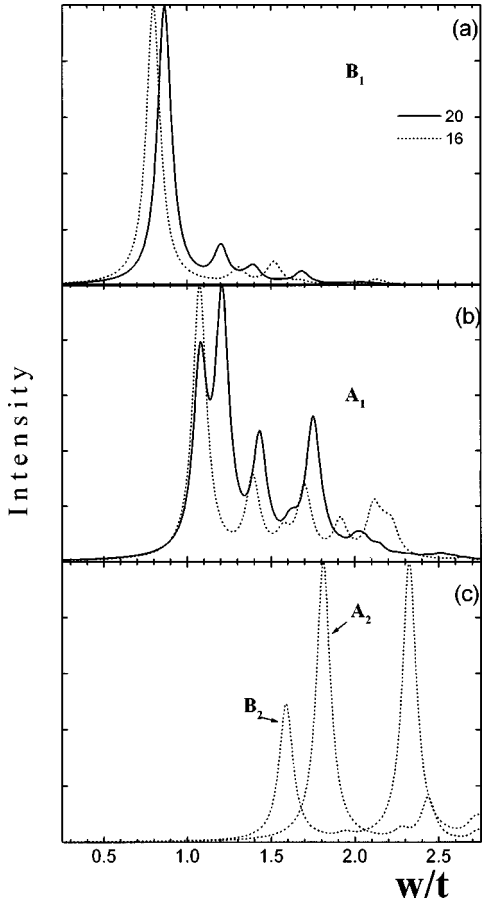

FIG. 1. B_{1g} and A_{1g} Raman spectra for 16 and 20 sites clusters. Calculations were done for the effective spin model with no spin-phonon interaction. The microscopic parameters correspond to $YBa_2Cu_3O_{6.2}$ (see Table I).

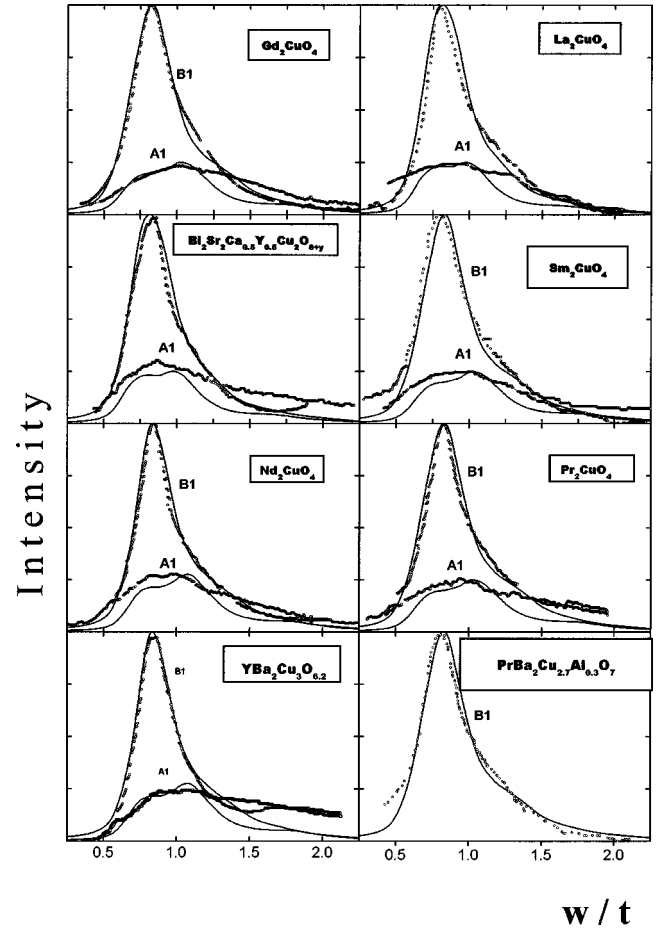

FIG. 2. B_{1g} and A_{1g} Raman spectra for the 20 sites cluster. The value of the parameters are given in Table I and $D=0.13$. Scattered symbols correspond to experimental data taken from Refs. 12–15, while solid lines are the result of theoretical calculations using the effective spin model taking into account fluctuations of the phonon field.

interaction. Indeed, infrared data for La_2CuO_4 gives frequencies of the O stretch modes as 550 and 690 cm^{-1}. This corresponds to a bond-stretching force constant K of ~ 7.5 and ~ 11 eV/Å^2, respectively,[43] i.e., $\sqrt{\langle x^2 \rangle} \sim 0.1$ Å. The electron-phonon interaction on the real material, modifies the exchange interaction parameter of the effective spin Hamiltonian *mainly* through the dependence of t_{pd} and the charge-transfer energy on the Cu-O distance $d_{\text{Cu-O}}$.[44] In the spin-wave approximation, the lowest order contribution to the damping of spin excitations due to the spin-phonon interaction is proportional to $|\nabla J|^2$.[45] Because along the M_2CuO_4 family, J changes almost linearly with $d_{\text{Cu-O}}$, $|\nabla J|$ takes the *constant* value ~ 4350 cm^{-1}/Å, so the maximum contribution to the exchange constant due to the spin-phonon coupling is $\Delta J \sim \pm 435$ cm^{-1}.

The spin-phonon interaction produces, through quantum fluctuations, some kind of dynamically induced disorder which can be seen by short-wavelength spin excitations. While the spin dynamic is driven by $\hbar\omega_s = J$, the phonon movement is by $\hbar\omega_{\text{ph}} \sim (20-60)$ meV$<J$, then in the spin system it appears that the oxygen atoms are frozen in different positions during *each* spin-exchange process. Since the phonon energy is much smaller than the exchange parameter, as a first approximation, the phonon energy can be taken as zero, then the spin-phonon interaction shows up through fluctuations of the phonon field. In this limit phonons can be modeled by static disorder,[46] in other words, the fluctuations of the phonon field can be modeled by a random distribution $P(J,D)$ of the exchange parameter of width D centered around J. For the one-band Hubbard model this correspond to a distribution for hoppings, centered around $t(t')$ with dispersion $Dt(Dt')$. In what follows we assume a Gaussian distribution for them. The value of D is of order $\lambda\sqrt{\langle x^2 \rangle}/t \sim (0.07-0.7)$ eV for an electron-phonon coupling $\lambda \sim (0.3-3.0)$.[43] Since the real value of D depends on the details of the microscopic model used for the planes as well as the material itself, we fixed $D=0.13$ which gives the better overall description of the mentioned insulators.

Figure 2 shows a comparison between experimental and calculated A_{1g} and B_{1g} spectra for seven different compounds. Table II presents the calculated and experimental values for the first two cumulants. All the spectra of Fig. 2 results from a quenched averaged over 150 samples. The calculated B_{1g} response shows many of the experimentally observed features. Indeed, the characteristic two-magnon peak is located at $\omega \sim 3J$, the spectra extend up to $8J$ and significant spectral weight is found at $\omega \sim (3.5-4)J$. The A_{1g} scattering appears in the same frequency range of the B_{1g} response $2J<\omega<4J$ and the center of gravity of this line is slightly shifted to the right with respect to the two-

TABLE II. Values of the cumulants M_1 and M_2 for Raman lines B_{1g} and A_{1g}. First lines correspond to experimental values taken from Refs. 12–15.

		YBaCuO	Pr_2CuO_4	Nd_2CuO_4	Sm_2CuO_4	La_2CuO_4	GdCuO	BSCYCO	PRBACAL
	M_1	1.11	1.01	1.03	1.00	0.96	0.97	0.95	0.93
		1.02	0.96	1.03	1.00	0.97	0.99	0.93	0.96
B_1	M_2	0.40	0.33	0.37	0.37	0.30	0.32	0.27	0.28
		0.42	0.30	0.39	0.40	0.38	0.42	0.27	0.30
	M_2/M_1	0.36	0.33	0.36	0.37	0.31	0.32	0.29	0.30
		0.41	0.31	0.39	0.40	0.39	0.42	0.29	0.31
	M_1	1.30	1.13	1.15	1.04	1.05	1.23	1.20	
		1.10	1.07	1.13	1.09	1.03	1.10	1.03	
A_1	M_2	0.42	0.39	0.45	0.37	0.38	0.42	0.46	
		0.35	0.33	0.37	0.36	0.33	0.37	0.35	
	M_2/M_1	0.32	0.35	0.39	0.36	0.36	0.34	0.39	
		0.32	0.30	0.33	0.33	0.32	0.33	0.34	

magnon peak. As it was stated in Ref. 14, the B_{1g} line can be well fitted with two Gaussian curves. One centered at $\omega \sim 3J$, and the other at $\omega \sim 4J$ with a relative intensity of 25% respect to the first one. Hence, from the explanation given above and the results presented in Ref. 31, it is clear that the Heisenberg model, even with the inclusion of spin-phonon interaction, cannot reproduce simultaneously the width and the asymmetry of the B_{1g} peak. It is necessary to take unrealistic values of disorder ($D=0.5J$) (Ref. 31) in order to transfer spectral weight from the two-magnon peak to higher energies. From Figs. 1 and 2, it becomes clear that the inclusion of additional terms (J' and K) are necessary to reproduce the whole shape of the B_{1g} line. These terms generate the whole structure of the A_{1g} line because O_{A_1} does not commute with the Heisenberg Hamiltonian. This structure has two main contributions of approximately the same weight. The first is the same as the two-magnon B_{1g} peak, now allowed in this representation due to the broken symmetry introduced by the fluctuations of the phonon field. Therefore, the intensity of this peak increases with D. The second contribution corresponds to four-magnon states [see Fig. 1(b)] mainly introduced by the J' and K terms of the Hamiltonian. Contrary to the B_{1g} contribution, this one does not have a regular behavior with D. If we depart from $D=0.13$ (the dispersion used to describe all B_{1g} lines) the two main A_{1g} peaks will not have the same intensity and the agreement with experiment will pair off. This point is clearly seen by comparing Fig. 2 with Fig. 1 of Ref. 31 where the A_{1g} line, using a Heisenberg model plus disorder, is given.

IV. SUMMARY

Summarizing, we have studied the role of spin-phonon and multispin interactions on the line shapes of light-scattering experiments within the Loudon-Fleury theory for the insulating cuprates. For the insulating parent materials of high-temperature superconductors, by contrast to conventional antiferromagnets, the energy of short-wavelength spin excitations is greater than the characteristic energy of optical phonons so a non-negligible contribution of the spin-phonon interaction is expected for the damping of spin excitations. Good qualitative agreement for the B_{1g} an the A_{1g} was found.

As it was noted before, to describe the dependence of the spectrum with the incident laser, a resonant theory should be used. But, as it was shown in a recent experiment on $PrBa_2Cu_{2.7}Al_{0.3}O_7$ (Ref. 16) (see Fig. 2), resonant effects become weak as the laser frequency is decreased. For low enough frequencies, the system is out of resonance. The main characteristics of the B_{1g} line measured in these conditions, the width of the main peak and the shoulder at higher energies, remain unaltered. By including spin-phonon interactions in the framework of the single-band Hubbard model we can reproduce quantitatively these features. The A_{1g} spectra are also well described within this theory. This is a theory with realistic parameters which can reproduce the B_{1g} and A_{1g} measured spectra. Therefore, we conclude that the Loudon-Fleury theory is a good starting point to describe the Raman spectra of the insulating cuprates.

In a recent work, a numerical calculation of the Heisenberg model in clusters as big as 6×6 was performed and two two-magnon peaks were found. If this is confirmed for bigger clusters (note that Monte Carlo max entropy calculations on bigger clusters do not show such structures), this could lower the phonon-magnon coupling needed to adjust the experiments. Unfortunately this is far from current numerical possibilities.

Finite-cluster calculations for eight insulating cuprates support the view of two contributing mechanisms to the B_{1g} and A_{1g} Raman lines. Although they contribute to different parts of the spectra, together they account for the enhanced linewidth and the asymmetry of the B_{1g} mode, as well as for a non-negligible response for the A_{1g} Raman line observed in these materials.

ACKNOWLEDGMENTS

We would like to thank E. Fradkin, R. M. Martin, and M. Klein for useful discussions at early stages of this work. All of us are supported by the Consejo Nacional de Investigaciones Científicas y Técnicas, Argentina. Partial support from Fundación Antorchas under Grant No. 13016/1 and from Agencia Nacional de Promoción Científica y Tecnológica under Grant No. PMT-PICT0005 are gratefully acknowledged.

[1] See, for example, S. Chakravarty, in *High Temperature Superconductivity*, edited by K. S. Bedell *et al.* (Addison-Wesley, Palo Alto CA, 1990); E. Manousakis, Rev. Mod. Phys. **63**, 1 (1991).
[2] P. A. Fleury and R. Loudon, Phys. Rev. **166**, 514 (1968).
[3] H.-Q. Ding and M. Makivic, Phys. Rev. Lett. **64**, 1449 (1990); M. Makivic and M. Jarrell, *ibid.* **68**, 1770 (1990).
[4] S. Chakravarty, B. I. Halperin, and D. R. Nelson, Phys. Rev. B **39**, 2344 (1989).
[5] A. Sokol, E. Gagliano, and S. Bacci, Phys. Rev. B **47**, 14 646 (1993).
[6] T. Imai *et al.*, Phys. Rev. Lett. **70**, 1002 (1993).
[7] R. R. P. Singh, P. A. Fleury, K. B. Lyons, and P. E. Sulewski, Phys. Rev. Lett. **62**, 2736 (1989).
[8] E. Gagliano and S. Bacci, Phys. Rev. B **42**, 8772 (1990); E. Dagotto and D. Poilblanc, *ibid.* **42**, 7940 (1990).
[9] Z. Liu and E. Manousakis, Phys. Rev. B **43**, 13 246 (1990).
[10] C. M. Canali and S. M. Girvin, Phys. Rev. B **45**, 7127 (1991).
[11] A. W. Sandvik, S. Capponi, D. Poilblanc, and E. Dagotto, Phys. Rev. B **57**, 8478 (1998).
[12] S. Sugai *et al.*, Phys. Rev. B **42**, 1045 (1990).
[13] P. E. Sulewski *et al.*, Phys. Rev. B **41**, 225 (1990).
[14] I. Tomeno *et al.*, Phys. Rev. B **43**, 3009 (1991).
[15] P. E. Sulewski *et al.*, Phys. Rev. Lett. **67**, 3864 (1991).
[16] M. Rübhausen, N. Dieckmann, A. Bock, and U. Merkt, Phys. Rev. B **54**, 14 967 (1996).
[17] For La_2CuO_4, see K. B. Lyons *et al.*, Phys. Rev. B **39**, 9693 (1989).
[18] P. E. Sulewski *et al.*, Phys. Rev. Lett. **67**, 3864 (1990).
[19] S. Bacci and E. Gagliano, Phys. Rev. B **43**, 6224 (1991).
[20] M. E. Simón, A. A. Aligia, C. D. Batista, E. R. Gagliano, and F. Lema, Phys. Rev. B **54**, R3780 (1996).
[21] Y. Y. Wang, F. C. Zhang, V. P. Dravid, K. K. Ng, M. V. Klein, S. E. Schnatterly, and L. L Miller, Phys. Rev. Lett. **77**, 1809 (1996).
[22] B. Beschoten, S. Sadewasser, G. Güntherodt, and C. Quitmann, Phys. Rev. Lett. **77**, 1837 (1996).
[23] A. V. Chubukov and D. M. Frenkel, Phys. Rev. Lett. **74**, 3057 (1995); Phys. Rev. B **52**, 9760 (1995).
[24] F. Schönfeld, A. P. Kampf, and E. Müller-Hartmann, Z. Phys. B **102**, 25 (1997).
[25] I. Ohana *et al.*, Phys. Rev. B **39**, 2293 (1989).
[26] G. Blumberg *et al.*, Phys. Rev. B **53**, 11 930 (1996).
[27] R. R. P. Singh, P. Prelovsek, and B. S. Shastry, Phys. Rev. Lett. **77**, 4086 (1996).
[28] C. Gross *et al.*, Phys. Rev. B **55**, 15 048 (1996).
[29] S. Rosenblum, A. H. Francis, and R. Merlin, Phys. Rev. B **49**, 4352 (1994).
[30] P. Knoll *et al.*, Phys. Rev. B **42**, 4842 (1990).
[31] F. Nori, R. Merlin, S. Haas, A. W. Sandvik, and E. Dagotto, Phys. Rev. Lett. **75**, 553 (1995).
[32] F. Lema, J. Eroles, C. Batista, and E. R. Gagliano, Phys. Rev. B **55**, 15 295 (1997).
[33] J. Lorenzana and G. A. Sawatzky, Phys. Rev. Lett. **74**, 186 (1995).
[34] E. Gagliano *et al.*, Phys. Rev. B **34**, 1677 (1986); E. Gagliano and C. Balseiro, Phys. Rev. Lett. **59**, 2999 (1987), and references therein.
[35] F. Nori, E. Gagliano, and S. Bacci, Phys. Rev. Lett. **68**, 240 (1992).
[36] B. Sriram Shastry and B. Shraiman, Phys. Rev. Lett. **65**, 1068 (1990).
[37] Calculations of the light-scattering spectrum for A_{2g} and B_{2g} show a very intensive peak located at $\omega \sim 6J$ and $\sim 6.5J$, respectively. See also, D. Poilblanc, E. Gagliano, S. Bacci, and E. Dagotto, Phys. Rev. B **43**, 10 970 (1991).
[38] H. J. Schmidt and Y. Kuramoto, Physica C **167**, 263 (1990).
[39] E. Gagliano, C. Balseiro, and M. Avignon, Europhys. Lett. **12**, 259 (1990); S. Bacci, E. Gagliano, and R. M. Martin, in *High-Temperature Superconductivity*, edited by J. Ashkenazi *et al.* (Plenum, New York, 1991).
[40] A. H. MacDonald, S. Girvin, and D. Yoshioka, Phys. Rev. B **41**, 2565 (1990).
[41] A. Chubukov, E. Gagliano, and C. Balseiro, Phys. Rev. B **45**, 7889 (1992).
[42] H. B. Schüttler and A. J. Fedro, Phys. Rev. B **45**, 7588 (1992); M. E. Simón and A. A. Aligia, *ibid.* **53**, 15 327 (1996); E. Dagotto, Rev. Mod. Phys. **66**, 763 (1994); M. E. Simón, A. A. Aligia, and E. R. Gagliano, Phys. Rev. B **56**, 5637 (1997).
[43] W. Weber, Phys. Rev. Lett. **58**, 1371 (1990); P. B. Allen, W. E. Pickett, and H. Krakauer, Phys. Rev. B **37**, 7482 (1988); R. Zeyher and G. Zwicknagle, Solid State Commun. **66**, 617 (1988).
[44] Y. Ohta *et al.*, Phys. Rev. Lett. **66**, 1228 (1991).
[45] M. G. Cottam, J. Phys. C **7**, 2901 (1974).
[46] M. J. Reilly and A. G. Rojo, Phys. Rev. B **53**, 6429 (1995).